

Measurement of the Decay $B^- \rightarrow D^{*0}e^-\bar{\nu}_e$

B. Aubert,¹ M. Bona,¹ D. Boutigny,¹ Y. Karyotakis,¹ J. P. Lees,¹ V. Poireau,¹ X. Prudent,¹ V. Tisserand,¹
A. Zghiche,¹ J. Garra Tico,² E. Grauges,² L. Lopez,³ A. Palano,³ M. Pappagallo,³ G. Eigen,⁴ B. Stugu,⁴
L. Sun,⁴ G. S. Abrams,⁵ M. Battaglia,⁵ D. N. Brown,⁵ J. Button-Shafer,⁵ R. N. Cahn,⁵ Y. Groyzman,⁵
R. G. Jacobsen,⁵ J. A. Kadyk,⁵ L. T. Kerth,⁵ Yu. G. Kolomensky,⁵ G. Kukartsev,⁵ D. Lopes Pegna,⁵ G. Lynch,⁵
L. M. Mir,⁵ T. J. Orimoto,⁵ I. L. Osipenkov,⁵ M. T. Ronan,^{5,*} K. Tackmann,⁵ T. Tanabe,⁵ W. A. Wenzel,⁵
P. del Amo Sanchez,⁶ C. M. Hawkes,⁶ A. T. Watson,⁶ T. Held,⁷ H. Koch,⁷ M. Pelizaeus,⁷ T. Schroeder,⁷
M. Steinke,⁷ D. Walker,⁸ D. J. Asgeirsson,⁹ T. Cuhadar-Donszelmann,⁹ B. G. Fulsom,⁹ C. Hearty,⁹ T. S. Mattison,⁹
J. A. McKenna,⁹ A. Khan,¹⁰ M. Saleem,¹⁰ L. Teodorescu,¹⁰ V. E. Blinov,¹¹ A. D. Bukin,¹¹ V. P. Druzhinin,¹¹
V. B. Golubev,¹¹ A. P. Onuchin,¹¹ S. I. Serednyakov,¹¹ Yu. I. Skovpen,¹¹ E. P. Solodov,¹¹ K. Yu. Todyshev,¹¹
M. Bondioli,¹² S. Curry,¹² I. Eschrich,¹² D. Kirkby,¹² A. J. Lankford,¹² P. Lund,¹² M. Mandelkern,¹²
E. C. Martin,¹² D. P. Stoker,¹² S. Abachi,¹³ C. Buchanan,¹³ S. D. Foulkes,¹⁴ J. W. Gary,¹⁴ F. Liu,¹⁴ O. Long,¹⁴
B. C. Shen,¹⁴ L. Zhang,¹⁴ H. P. Paar,¹⁵ S. Rahatlou,¹⁵ V. Sharma,¹⁵ J. W. Berryhill,¹⁶ C. Campagnari,¹⁶
A. Cunha,¹⁶ B. Dahmes,¹⁶ T. M. Hong,¹⁶ D. Kovalskyi,¹⁶ J. D. Richman,¹⁶ T. W. Beck,¹⁷ A. M. Eisner,¹⁷
C. J. Flacco,¹⁷ C. A. Heusch,¹⁷ J. Kroseberg,¹⁷ W. S. Lockman,¹⁷ T. Schalk,¹⁷ B. A. Schumm,¹⁷ A. Seiden,¹⁷
M. G. Wilson,¹⁷ L. O. Winstrom,¹⁷ E. Chen,¹⁸ C. H. Cheng,¹⁸ F. Fang,¹⁸ D. G. Hitlin,¹⁸ I. Narsky,¹⁸ T. Piatenko,¹⁸
F. C. Porter,¹⁸ R. Andreassen,¹⁹ G. Mancinelli,¹⁹ B. T. Meadows,¹⁹ K. Mishra,¹⁹ M. D. Sokoloff,¹⁹ F. Blanc,²⁰
P. C. Bloom,²⁰ S. Chen,²⁰ W. T. Ford,²⁰ J. F. Hirschauer,²⁰ A. Kreisel,²⁰ M. Nagel,²⁰ U. Nauenberg,²⁰ A. Olivas,²⁰
J. G. Smith,²⁰ K. A. Ulmer,²⁰ S. R. Wagner,²⁰ J. Zhang,²⁰ A. M. Gabareen,²¹ A. Soffer,^{21,†} W. H. Toki,²¹
R. J. Wilson,²¹ F. Winklmeier,²¹ D. D. Altenburg,²² E. Feltresi,²² A. Hauke,²² H. Jasper,²² J. Merkel,²²
A. Petzold,²² B. Spaan,²² K. Wacker,²² V. Klose,²³ M. J. Kobel,²³ H. M. Lacker,²³ W. F. Mader,²³ R. Nogowski,²³
J. Schubert,²³ K. R. Schubert,²³ R. Schwierz,²³ J. E. Sundermann,²³ A. Volk,²³ D. Bernard,²⁴ G. R. Bonneaud,²⁴
E. Latour,²⁴ V. Lombardo,²⁴ Ch. Thiebaux,²⁴ M. Verderi,²⁴ P. J. Clark,²⁵ W. Gradl,²⁵ F. Muheim,²⁵ S. Playfer,²⁵
A. I. Robertson,²⁵ J. E. Watson,²⁵ Y. Xie,²⁵ M. Andreotti,²⁶ D. Bettoni,²⁶ C. Bozzi,²⁶ R. Calabrese,²⁶ A. Cecchi,²⁶
G. Cibinetto,²⁶ P. Franchini,²⁶ E. Luppi,²⁶ M. Negrini,²⁶ A. Petrella,²⁶ L. Piemontese,²⁶ E. Prencipe,²⁶
V. Santoro,²⁶ F. Anulli,²⁷ R. Baldini-Ferrolì,²⁷ A. Calcaterra,²⁷ R. de Sangro,²⁷ G. Finocchiaro,²⁷ S. Pacetti,²⁷
P. Patteri,²⁷ I. M. Peruzzi,^{27,‡} M. Piccolo,²⁷ M. Rama,²⁷ A. Zallo,²⁷ A. Buzzo,²⁸ R. Contri,²⁸ M. Lo Vetere,²⁸
M. M. Macri,²⁸ M. R. Monge,²⁸ S. Passaggio,²⁸ C. Patrignani,²⁸ E. Robutti,²⁸ A. Santroni,²⁸ S. Tosi,²⁸
K. S. Chaisanguanthum,²⁹ M. Morii,²⁹ J. Wu,²⁹ R. S. Dubitzky,³⁰ J. Marks,³⁰ S. Schenk,³⁰ U. Uwer,³⁰ D. J. Bard,³¹
P. D. Dauncey,³¹ R. L. Flack,³¹ J. A. Nash,³¹ W. Panduro Vazquez,³¹ M. Tibbetts,³¹ P. K. Behera,³² X. Chai,³²
M. J. Charles,³² U. Mallik,³² V. Ziegler,³² J. Cochran,³³ H. B. Crawley,³³ L. Dong,³³ V. Eyges,³³ W. T. Meyer,³³
S. Prell,³³ E. I. Rosenberg,³³ A. E. Rubin,³³ Y. Y. Gao,³⁴ A. V. Gritsan,³⁴ Z. J. Guo,³⁴ C. K. Lae,³⁴ A. G. Denig,³⁵
M. Fritsch,³⁵ G. Schott,³⁵ N. Arnaud,³⁶ J. Béquilleux,³⁶ A. D’Orazio,³⁶ M. Davier,³⁶ G. Grosdidier,³⁶ A. Höcker,³⁶
V. Lepeltier,³⁶ F. Le Diberder,³⁶ A. M. Lutz,³⁶ S. Pruvot,³⁶ S. Rodier,³⁶ P. Roudeau,³⁶ M. H. Schune,³⁶
J. Serrano,³⁶ V. Sordini,³⁶ A. Stocchi,³⁶ W. F. Wang,³⁶ G. Wormser,³⁶ D. J. Lange,³⁷ D. M. Wright,³⁷
I. Bingham,³⁸ C. A. Chavez,³⁸ I. J. Forster,³⁸ J. R. Fry,³⁸ E. Gabathuler,³⁸ R. Gamet,³⁸ D. E. Hutchcroft,³⁸
D. J. Payne,³⁸ K. C. Schofield,³⁸ C. Touramanis,³⁸ A. J. Bevan,³⁹ K. A. George,³⁹ F. Di Lodovico,³⁹ W. Menges,³⁹
R. Sacco,³⁹ G. Cowan,⁴⁰ H. U. Flaecher,⁴⁰ D. A. Hopkins,⁴⁰ S. Paramesvaran,⁴⁰ F. Salvatore,⁴⁰ A. C. Wren,⁴⁰
D. N. Brown,⁴¹ C. L. Davis,⁴¹ J. Allison,⁴² N. R. Barlow,⁴² R. J. Barlow,⁴² Y. M. Chia,⁴² C. L. Edgar,⁴²
G. D. Lafferty,⁴² T. J. West,⁴² J. I. Yi,⁴² J. Anderson,⁴³ C. Chen,⁴³ A. Jawahery,⁴³ D. A. Roberts,⁴³ G. Simi,⁴³
J. M. Tuggle,⁴³ G. Blaylock,⁴⁴ C. Dallapiccola,⁴⁴ S. S. Hertzbach,⁴⁴ X. Li,⁴⁴ T. B. Moore,⁴⁴ E. Salvati,⁴⁴
S. Saremi,⁴⁴ R. Cowan,⁴⁵ D. Dujmic,⁴⁵ P. H. Fisher,⁴⁵ K. Koeneke,⁴⁵ G. Sciolla,⁴⁵ S. J. Sekula,⁴⁵ M. Spitznagel,⁴⁵
F. Taylor,⁴⁵ R. K. Yamamoto,⁴⁵ M. Zhao,⁴⁵ Y. Zheng,⁴⁵ S. E. Mclachlin,^{46,*} P. M. Patel,⁴⁶ S. H. Robertson,⁴⁶
A. Lazzaro,⁴⁷ F. Palombo,⁴⁷ J. M. Bauer,⁴⁸ L. Cremaldi,⁴⁸ V. Eschenburg,⁴⁸ R. Godang,⁴⁸ R. Kroeger,⁴⁸
D. A. Sanders,⁴⁸ D. J. Summers,⁴⁸ H. W. Zhao,⁴⁸ S. Brunet,⁴⁹ D. Côté,⁴⁹ M. Simard,⁴⁹ P. Taras,⁴⁹ F. B. Viaud,⁴⁹
H. Nicholson,⁵⁰ G. De Nardo,⁵¹ F. Fabozzi,^{51,§} L. Lista,⁵¹ D. Monorchio,⁵¹ C. Sciacca,⁵¹ M. A. Baak,⁵² G. Raven,⁵²
H. L. Snoek,⁵² C. P. Jessop,⁵³ K. J. Knoepfel,⁵³ J. M. LoSecco,⁵³ G. Benelli,⁵⁴ L. A. Corwin,⁵⁴ K. Honscheid,⁵⁴

H. Kagan,⁵⁴ R. Kass,⁵⁴ J. P. Morris,⁵⁴ A. M. Rahimi,⁵⁴ J. J. Regensburger,⁵⁴ Q. K. Wong,⁵⁴ N. L. Blount,⁵⁵ J. Brau,⁵⁵ R. Frey,⁵⁵ O. Igonkina,⁵⁵ J. A. Kolb,⁵⁵ M. Lu,⁵⁵ R. Rahmat,⁵⁵ N. B. Sinev,⁵⁵ D. Strom,⁵⁵ J. Strube,⁵⁵ E. Torrence,⁵⁵ N. Gagliardi,⁵⁶ A. Gaz,⁵⁶ M. Margoni,⁵⁶ M. Morandin,⁵⁶ A. Pompili,⁵⁶ M. Posocco,⁵⁶ M. Rotondo,⁵⁶ F. Simonetto,⁵⁶ R. Stroili,⁵⁶ C. Voci,⁵⁶ E. Ben-Haim,⁵⁷ H. Briand,⁵⁷ G. Calderini,⁵⁷ J. Chauveau,⁵⁷ P. David,⁵⁷ L. Del Buono,⁵⁷ Ch. de la Vaissière,⁵⁷ O. Hamon,⁵⁷ Ph. Leruste,⁵⁷ J. Malclès,⁵⁷ J. Ocariz,⁵⁷ A. Perez,⁵⁷ J. Prendki,⁵⁷ L. Gladney,⁵⁸ M. Biasini,⁵⁹ R. Covarelli,⁵⁹ E. Manoni,⁵⁹ C. Angelini,⁶⁰ G. Batignani,⁶⁰ S. Bettarini,⁶⁰ M. Carpinelli,⁶⁰ R. Cenci,⁶⁰ A. Cervelli,⁶⁰ F. Forti,⁶⁰ M. A. Giorgi,⁶⁰ A. Lusiani,⁶⁰ G. Marchiori,⁶⁰ M. A. Mazur,⁶⁰ M. Morganti,⁶⁰ N. Neri,⁶⁰ E. Paoloni,⁶⁰ G. Rizzo,⁶⁰ J. J. Walsh,⁶⁰ M. Haire,⁶¹ J. Biesiada,⁶² P. Elmer,⁶² Y. P. Lau,⁶² C. Lu,⁶² J. Olsen,⁶² A. J. S. Smith,⁶² A. V. Telnov,⁶² E. Baracchini,⁶³ F. Bellini,⁶³ G. Cavoto,⁶³ D. del Re,⁶³ E. Di Marco,⁶³ R. Faccini,⁶³ F. Ferrarotto,⁶³ F. Ferroni,⁶³ M. Gaspero,⁶³ P. D. Jackson,⁶³ L. Li Gioi,⁶³ M. A. Mazzoni,⁶³ S. Morganti,⁶³ G. Piredda,⁶³ F. Polci,⁶³ F. Renga,⁶³ C. Voena,⁶³ M. Ebert,⁶⁴ T. Hartmann,⁶⁴ H. Schröder,⁶⁴ R. Waldi,⁶⁴ T. Adye,⁶⁵ G. Castelli,⁶⁵ B. Franek,⁶⁵ E. O. Olaiya,⁶⁵ S. Ricciardi,⁶⁵ W. Roethel,⁶⁵ F. F. Wilson,⁶⁵ S. Emery,⁶⁶ M. Escalier,⁶⁶ A. Gaidot,⁶⁶ S. F. Ganzhur,⁶⁶ G. Hamel de Monchenault,⁶⁶ W. Kozanecki,⁶⁶ G. Vasseur,⁶⁶ Ch. Yèche,⁶⁶ M. Zito,⁶⁶ X. R. Chen,⁶⁷ H. Liu,⁶⁷ W. Park,⁶⁷ M. V. Purohit,⁶⁷ J. R. Wilson,⁶⁷ M. T. Allen,⁶⁸ D. Aston,⁶⁸ R. Bartoldus,⁶⁸ P. Bechtle,⁶⁸ N. Berger,⁶⁸ R. Claus,⁶⁸ J. P. Coleman,⁶⁸ M. R. Convery,⁶⁸ J. C. Dingfelder,⁶⁸ J. Dorfan,⁶⁸ G. P. Dubois-Felsmann,⁶⁸ W. Dunwoodie,⁶⁸ R. C. Field,⁶⁸ T. Glanzman,⁶⁸ S. J. Gowdy,⁶⁸ M. T. Graham,⁶⁸ P. Grenier,⁶⁸ C. Hast,⁶⁸ T. Hryn'ova,⁶⁸ W. R. Innes,⁶⁸ J. Kaminski,⁶⁸ M. H. Kelsey,⁶⁸ H. Kim,⁶⁸ P. Kim,⁶⁸ M. L. Kocian,⁶⁸ D. W. G. S. Leith,⁶⁸ S. Li,⁶⁸ S. Luitz,⁶⁸ V. Luth,⁶⁸ H. L. Lynch,⁶⁸ D. B. MacFarlane,⁶⁸ H. Marsiske,⁶⁸ R. Messner,⁶⁸ D. R. Muller,⁶⁸ C. P. O'Grady,⁶⁸ I. Ofte,⁶⁸ A. Perazzo,⁶⁸ M. Perl,⁶⁸ T. Pulliam,⁶⁸ B. N. Ratcliff,⁶⁸ A. Roodman,⁶⁸ A. A. Salnikov,⁶⁸ R. H. Schindler,⁶⁸ J. Schwiening,⁶⁸ A. Snyder,⁶⁸ J. Stelzer,⁶⁸ D. Su,⁶⁸ M. K. Sullivan,⁶⁸ K. Suzuki,⁶⁸ S. K. Swain,⁶⁸ J. M. Thompson,⁶⁸ J. Va'vra,⁶⁸ N. van Bakel,⁶⁸ A. P. Wagner,⁶⁸ M. Weaver,⁶⁸ W. J. Wisniewski,⁶⁸ M. Wittgen,⁶⁸ D. H. Wright,⁶⁸ A. K. Yarritu,⁶⁸ K. Yi,⁶⁸ C. C. Young,⁶⁸ P. R. Burchat,⁶⁹ A. J. Edwards,⁶⁹ S. A. Majewski,⁶⁹ B. A. Petersen,⁶⁹ L. Wilden,⁶⁹ S. Ahmed,⁷⁰ M. S. Alam,⁷⁰ R. Bula,⁷⁰ J. A. Ernst,⁷⁰ V. Jain,⁷⁰ B. Pan,⁷⁰ M. A. Saeed,⁷⁰ F. R. Wappler,⁷⁰ S. B. Zain,⁷⁰ M. Krishnamurthy,⁷¹ S. M. Spanier,⁷¹ R. Eckmann,⁷² J. L. Ritchie,⁷² A. M. Ruland,⁷² C. J. Schilling,⁷² R. F. Schwitters,⁷² J. M. Izen,⁷³ X. C. Lou,⁷³ S. Ye,⁷³ F. Bianchi,⁷⁴ F. Gallo,⁷⁴ D. Gamba,⁷⁴ M. Pelliccioni,⁷⁴ M. Bomben,⁷⁵ L. Bosisio,⁷⁵ C. Cartaro,⁷⁵ F. Cossutti,⁷⁵ G. Della Ricca,⁷⁵ L. Lanceri,⁷⁵ L. Vitale,⁷⁵ V. Azzolini,⁷⁶ N. Lopez-March,⁷⁶ F. Martinez-Vidal,⁷⁶ D. A. Milanes,⁷⁶ A. Oyangueren,⁷⁶ J. Albert,⁷⁷ Sw. Banerjee,⁷⁷ B. Bhuyan,⁷⁷ K. Hamano,⁷⁷ R. Kowalewski,⁷⁷ I. M. Nugent,⁷⁷ J. M. Roney,⁷⁷ R. J. Sobie,⁷⁷ P. F. Harrison,⁷⁸ J. Ilic,⁷⁸ T. E. Latham,⁷⁸ G. B. Mohanty,⁷⁸ H. R. Band,⁷⁹ X. Chen,⁷⁹ S. Dasu,⁷⁹ K. T. Flood,⁷⁹ J. J. Hollar,⁷⁹ P. E. Kutter,⁷⁹ Y. Pan,⁷⁹ M. Pierini,⁷⁹ R. Prepost,⁷⁹ S. L. Wu,⁷⁹ and H. Neal⁸⁰

(The BABAR Collaboration)

¹Laboratoire de Physique des Particules, IN2P3/CNRS et Université de Savoie, F-74941 Annecy-Le-Vieux, France

²Universitat de Barcelona, Facultat de Física, Departament ECM, E-08028 Barcelona, Spain

³Università di Bari, Dipartimento di Fisica and INFN, I-70126 Bari, Italy

⁴University of Bergen, Institute of Physics, N-5007 Bergen, Norway

⁵Lawrence Berkeley National Laboratory and University of California, Berkeley, California 94720, USA

⁶University of Birmingham, Birmingham, B15 2TT, United Kingdom

⁷Ruhr Universität Bochum, Institut für Experimentalphysik 1, D-44780 Bochum, Germany

⁸University of Bristol, Bristol BS8 1TL, United Kingdom

⁹University of British Columbia, Vancouver, British Columbia, Canada V6T 1Z1

¹⁰Brunel University, Uxbridge, Middlesex UB8 3PH, United Kingdom

¹¹Budker Institute of Nuclear Physics, Novosibirsk 630090, Russia

¹²University of California at Irvine, Irvine, California 92697, USA

¹³University of California at Los Angeles, Los Angeles, California 90024, USA

¹⁴University of California at Riverside, Riverside, California 92521, USA

¹⁵University of California at San Diego, La Jolla, California 92093, USA

¹⁶University of California at Santa Barbara, Santa Barbara, California 93106, USA

¹⁷University of California at Santa Cruz, Institute for Particle Physics, Santa Cruz, California 95064, USA

¹⁸California Institute of Technology, Pasadena, California 91125, USA

¹⁹University of Cincinnati, Cincinnati, Ohio 45221, USA

²⁰University of Colorado, Boulder, Colorado 80309, USA

²¹Colorado State University, Fort Collins, Colorado 80523, USA

²²Universität Dortmund, Institut für Physik, D-44221 Dortmund, Germany

²³Technische Universität Dresden, Institut für Kern- und Teilchenphysik, D-01062 Dresden, Germany

²⁴Laboratoire Leprince-Ringuet, CNRS/IN2P3, Ecole Polytechnique, F-91128 Palaiseau, France

- ²⁵ University of Edinburgh, Edinburgh EH9 3JZ, United Kingdom
- ²⁶ Università di Ferrara, Dipartimento di Fisica and INFN, I-44100 Ferrara, Italy
- ²⁷ Laboratori Nazionali di Frascati dell'INFN, I-00044 Frascati, Italy
- ²⁸ Università di Genova, Dipartimento di Fisica and INFN, I-16146 Genova, Italy
- ²⁹ Harvard University, Cambridge, Massachusetts 02138, USA
- ³⁰ Universität Heidelberg, Physikalisches Institut, Philosophenweg 12, D-69120 Heidelberg, Germany
- ³¹ Imperial College London, London, SW7 2AZ, United Kingdom
- ³² University of Iowa, Iowa City, Iowa 52242, USA
- ³³ Iowa State University, Ames, Iowa 50011-3160, USA
- ³⁴ Johns Hopkins University, Baltimore, Maryland 21218, USA
- ³⁵ Universität Karlsruhe, Institut für Experimentelle Kernphysik, D-76021 Karlsruhe, Germany
- ³⁶ Laboratoire de l'Accélérateur Linéaire, IN2P3/CNRS et Université Paris-Sud 11, Centre Scientifique d'Orsay, B. P. 34, F-91898 ORSAY Cedex, France
- ³⁷ Lawrence Livermore National Laboratory, Livermore, California 94550, USA
- ³⁸ University of Liverpool, Liverpool L69 7ZE, United Kingdom
- ³⁹ Queen Mary, University of London, E1 4NS, United Kingdom
- ⁴⁰ University of London, Royal Holloway and Bedford New College, Egham, Surrey TW20 0EX, United Kingdom
- ⁴¹ University of Louisville, Louisville, Kentucky 40292, USA
- ⁴² University of Manchester, Manchester M13 9PL, United Kingdom
- ⁴³ University of Maryland, College Park, Maryland 20742, USA
- ⁴⁴ University of Massachusetts, Amherst, Massachusetts 01003, USA
- ⁴⁵ Massachusetts Institute of Technology, Laboratory for Nuclear Science, Cambridge, Massachusetts 02139, USA
- ⁴⁶ McGill University, Montréal, Québec, Canada H3A 2T8
- ⁴⁷ Università di Milano, Dipartimento di Fisica and INFN, I-20133 Milano, Italy
- ⁴⁸ University of Mississippi, University, Mississippi 38677, USA
- ⁴⁹ Université de Montréal, Physique des Particules, Montréal, Québec, Canada H3C 3J7
- ⁵⁰ Mount Holyoke College, South Hadley, Massachusetts 01075, USA
- ⁵¹ Università di Napoli Federico II, Dipartimento di Scienze Fisiche and INFN, I-80126, Napoli, Italy
- ⁵² NIKHEF, National Institute for Nuclear Physics and High Energy Physics, NL-1009 DB Amsterdam, The Netherlands
- ⁵³ University of Notre Dame, Notre Dame, Indiana 46556, USA
- ⁵⁴ Ohio State University, Columbus, Ohio 43210, USA
- ⁵⁵ University of Oregon, Eugene, Oregon 97403, USA
- ⁵⁶ Università di Padova, Dipartimento di Fisica and INFN, I-35131 Padova, Italy
- ⁵⁷ Laboratoire de Physique Nucléaire et de Hautes Energies, IN2P3/CNRS, Université Pierre et Marie Curie-Paris6, Université Denis Diderot-Paris7, F-75252 Paris, France
- ⁵⁸ University of Pennsylvania, Philadelphia, Pennsylvania 19104, USA
- ⁵⁹ Università di Perugia, Dipartimento di Fisica and INFN, I-06100 Perugia, Italy
- ⁶⁰ Università di Pisa, Dipartimento di Fisica, Scuola Normale Superiore and INFN, I-56127 Pisa, Italy
- ⁶¹ Prairie View A&M University, Prairie View, Texas 77446, USA
- ⁶² Princeton University, Princeton, New Jersey 08544, USA
- ⁶³ Università di Roma La Sapienza, Dipartimento di Fisica and INFN, I-00185 Roma, Italy
- ⁶⁴ Universität Rostock, D-18051 Rostock, Germany
- ⁶⁵ Rutherford Appleton Laboratory, Chilton, Didcot, Oxon, OX11 0QX, United Kingdom
- ⁶⁶ DSM/Dapnia, CEA/Saclay, F-91191 Gif-sur-Yvette, France
- ⁶⁷ University of South Carolina, Columbia, South Carolina 29208, USA
- ⁶⁸ Stanford Linear Accelerator Center, Stanford, California 94309, USA
- ⁶⁹ Stanford University, Stanford, California 94305-4060, USA
- ⁷⁰ State University of New York, Albany, New York 12222, USA
- ⁷¹ University of Tennessee, Knoxville, Tennessee 37996, USA
- ⁷² University of Texas at Austin, Austin, Texas 78712, USA
- ⁷³ University of Texas at Dallas, Richardson, Texas 75083, USA
- ⁷⁴ Università di Torino, Dipartimento di Fisica Sperimentale and INFN, I-10125 Torino, Italy
- ⁷⁵ Università di Trieste, Dipartimento di Fisica and INFN, I-34127 Trieste, Italy
- ⁷⁶ IFIC, Universitat de Valencia-CSIC, E-46071 Valencia, Spain
- ⁷⁷ University of Victoria, Victoria, British Columbia, Canada V8W 3P6
- ⁷⁸ Department of Physics, University of Warwick, Coventry CV4 7AL, United Kingdom
- ⁷⁹ University of Wisconsin, Madison, Wisconsin 53706, USA
- ⁸⁰ Yale University, New Haven, Connecticut 06511, USA

(Dated: September 19, 2021)

Using 226 million $B\bar{B}$ events recorded on the $\Upsilon(4S)$ resonance with the BABAR detector at the SLAC e^+e^- storage rings PEP-II, we reconstruct $B^- \rightarrow D^{*0}e^-\bar{\nu}_e$ decays using the decay chain $D^{*0} \rightarrow D^0\pi^0$ and $D^0 \rightarrow K^-\pi^+$. From the dependence of their differential rate on w , the product of

the four-velocities of B^- and D^{*0} , and using the description of the form factor $F(w)$ by Caprini et al., we obtain the preliminary results $\rho_{A_1}^2 = 1.15 \pm 0.06 \pm 0.08$, $F(1) \cdot |V_{cb}| = (36.3 \pm 0.6 \pm 1.4) \cdot 10^{-3}$, and $\mathcal{B}(B^- \rightarrow D^{*0} e^- \bar{\nu}_e) = (5.71 \pm 0.08 \pm 0.41)\%$. The first errors are statistical and the second ones are systematic.

*Submitted to the 2007 Europhysics Conference on High Energy Physics,
Manchester, England.*

PACS numbers: 13.25.Hw, 12.15.Hh, 11.30.Er

The exclusive B -meson decay modes with the highest rates are the two semileptonic modes $\bar{B}^0 \rightarrow D^{*+} e^- \bar{\nu}_e$ and $B^- \rightarrow D^{*0} e^- \bar{\nu}_e$. Whereas the first has been measured by many experiments [1] to determine its rate Γ , its differential rate $d\Gamma/dw$, and the CKM matrix element $|V_{cb}|$, the second has only been measured by two groups [2, 3] with lower statistics. In the B^0 mode, the observed differential decay rate is well described by heavy-quark effective QCD (HQET) using form factors with the slope parameter ρ^2 . However, the B^0 experiments do not agree well in their ρ^2 results. Using the isospin symmetry $d\Gamma(B^- \rightarrow D^{*0} e^- \bar{\nu}_e) = d\Gamma(\bar{B}^0 \rightarrow D^{*+} e^- \bar{\nu}_e)$, a precision measurement for the B^- mode can help to improve knowledge of ρ^2 and consequently of Γ and $|V_{cb}|$.

The aim of our analysis [4] is the determination of the differential decay fraction $d\mathcal{B}/dw(B^- \rightarrow D^{*0} e^- \bar{\nu}_e)$,

where \mathcal{B} is related to the decay rate Γ by the known lifetime $\tau(B^-)$ and w is the invariant product of the four-velocities of B^- and D^{*0} . The neutrino in the $B^- \rightarrow D^{*0} e^- \bar{\nu}_e$ decay is not reconstructed. Therefore, the w value of each reconstructed event cannot be obtained, only an approximation \tilde{w} which will be defined below. Instead of unfolding, the parametrized $d\mathcal{B}/d\tilde{w}$ expectation together with the w resolution from Monte Carlo simulation (MC) is fitted to the observed $d\mathcal{B}/d\tilde{w}$ distribution. Our fit, as in other recent $B^0 \rightarrow D^* \ell \nu$ analyses, uses the parametrization of Caprini et al. [5] and determines the two parameters $F(1) \cdot |V_{cb}|$ and ρ^2 . The third result, $\mathcal{B}(B^- \rightarrow D^{*0} e^- \bar{\nu}_e)$, is obtained by integrating $d\mathcal{B}/w$. The parametrization is defined by the following expressions:

$$\begin{aligned} \frac{d\Gamma(B^- \rightarrow D^{*0} e^- \bar{\nu}_e)}{dw} &= \frac{G_F^2}{48\pi^3} (m_B - m_{D^*})^2 m_{D^*}^3 \sqrt{w^2 - 1} (w + 1)^2 \\ &\times \left[1 + \frac{4w}{w + 1} \frac{m_B^2 - 2wm_B m_{D^*} + m_{D^*}^2}{(m_B - m_{D^*})^2} \right] \cdot F(w)^2 |V_{cb}|^2, \\ F(w)^2 &= |h_{A_1}(w)|^2 \left[1 + \frac{4w}{w + 1} \frac{m_B^2 - 2wm_B m_{D^*} + m_{D^*}^2}{(m_B - m_{D^*})^2} \right]^{-1} \sum_{i=0,+,-} |\tilde{H}_i(w)|^2, \\ |\tilde{H}_0(w)|^2 &= \left[1 + \frac{w - 1}{1 - r} (1 - R_2(w)) \right]^2, \quad |\tilde{H}_\pm(w)|^2 = \frac{1 - 2wr + r^2}{(1 - r)^2} \left[1 \mp \sqrt{\frac{w - 1}{w + 1}} R_1(w) \right]^2, \\ \frac{h_{A_1}(w)}{h_{A_1}(1)} &= 1 - 8\rho_{A_1}^2 z + (53\rho_{A_1}^2 - 15) z^2 - (231\rho_{A_1}^2 - 91) z^3, \quad z = \frac{\sqrt{w + 1} - \sqrt{2}}{\sqrt{w + 1} + \sqrt{2}}, \\ R_1(w) &= R_1(1) - 0.12(w - 1) + 0.05(w - 1)^2, \quad R_2(w) = R_2(1) + 0.11(w - 1) - 0.06(w - 1)^2. \end{aligned}$$

Note that $\rho^2 = \rho_{A_1}^2$ in this notation. The parameters $R_1(1)$ and $R_2(1)$ are not determined in this analysis; we use the *BABAR* results from the $\bar{B}^0 \rightarrow D^* \ell \nu$ decay as input, see [6] and Table I.

For our analysis, we use 205 fb^{-1} of e^+e^- annihilation data recorded at $\sqrt{s} \approx m(\Upsilon(4S))$ with the *BABAR* detector [7] at the SLAC storage rings PEP-II [8]. In addition to these on-peak data, we also use 16 fb^{-1} of

off-peak data collected below the $\Upsilon(4S)$ resonance. We select $B^- \rightarrow D^{*0}e^- \bar{\nu}_e$ candidates [9] by pairing electrons with $p^* > 1.2 \text{ GeV}/c$ in the e^+e^- rest frame with D^{*0} candidates. Since the precision of our results is not limited by statistics, we restrict the analysis to the sequential decay modes $D^{*0} \rightarrow D^0\pi^0$ and $D^0 \rightarrow K^-\pi^+$, which have the smallest combinatorial background and the best resolution in $\Delta m \equiv m(K^-\pi^+\pi^0) - m(K^-\pi^+)$.

Charged particles are selected if they have at least 10 hits in the *BABAR* drift chamber, transverse momentum $p_T > 0.1 \text{ GeV}/c$, and a polar angle between 23.5° and 145.5° . Electrons (kaons) are selected with tight (loose) *BABAR* particle identification criteria. Neutral pions are reconstructed from two photons with energy above 30 MeV and a photon-compatible lateral shower shape in the *BABAR* calorimeter. The invariant mass must be $115 < m_{\gamma\gamma} < 150 \text{ MeV}/c^2$, and the photon pair is then constrained to a common vertex and to $m_{\gamma\gamma} = m(\pi^0)$. The decay candidates have to fulfill the following further requirements: The D^{*0} - D^0 mass difference must be $135 < \Delta m < 153 \text{ MeV}/c^2$ and the D^0 -candidate mass $1.8496 < m(K^-\pi^+) < 1.8796 \text{ GeV}/c^2$. To reject non- B -decay candidates, the normalized Fox-Wolfram moment R_2 [10] of the event has to be smaller than 0.45. To reject candidates with a D^{*0} from one B meson and an electron from the other B in the event, the angle between the D^{*0} and the e^- has to be larger than 90° .

Since there are many low-energy background photons, the selection criteria result in many events with two or more $D^{*0}e$ candidates, on average 1.75 per event. All $D^{*0}e$ candidates in the same $eK\pi$ combination are collected into one candidate group; on average there are 1.015 candidate groups per event. Only one candidate group per event is kept, in case of multiple groups the one with the smallest deviation $|m(K\pi) - m(D^0)|$. All candidates in one group are kept in the analysis because the simulation of low-energy photons is not perfect. This procedure ensures that correctly reconstructed candidates are selected with the same probability in data and MC.

The set of surviving candidates is binned in three dimensions according to their values of Δm , $\cos\theta_{\text{BY}}^*$, and \tilde{w} . The first two variables are used for the separation between signal and background, the third is used for the w dependence of the signal. Δm is defined above, and θ_{BY}^* is the angle between the directions of the B meson and the $Y = D^{*0} + e$ system in the e^+e^- rest frame under the hypothesis that the B decays into only D^{*0} , e , and neutrino. It is defined by the four-vector relation

$$p_\nu^2 = 0 = m_B^2 + m_Y^2 - 2(E_B^* E_Y^* - |\vec{p}_B^*| |\vec{p}_Y^*| \cos\theta_{\text{BY}}^*).$$

The value of

$$w = w(\beta^*) \equiv \frac{E_B^* E_{D^*} - |\vec{p}_B^*| |\vec{p}_{D^*}^*| \cos\beta^*}{m_B m_{D^*}}$$

cannot be determined since the angle β^* between the B and the D^{*0} in the e^+e^- rest frame is unknown. However,

β^* is bound between a minimum and a maximum value, and

$$\tilde{w} = [w(\beta_{\text{min}}^*) + w(\beta_{\text{max}}^*)]/2$$

is a good estimator for w in each event. w and \tilde{w} span a range from 1 to 1.5, the distribution of $\tilde{w} - w$ is nearly Gaussian with an RMS of 0.026. We use 10 equidistant bins of \tilde{w} , their width corresponds to about 2 RMS.

The fit for the two parameters $V = F(1)|V_{cb}|$ and ρ^2 is a binned maximum-likelihood fit in three dimensions. The fit function is the sum of the expected signal function $S = S(V, \rho^2)$ and the various expected background functions. The signal function in each \tilde{w} bin is taken as the product of one-dimensional functions of Δm and $\cos\theta_{\text{BY}}^*$. These two functions are obtained from fits to the reweighted signal MC distributions with V^- , ρ^2 -, $R_1(1)$ -, and $R_2(1)$ -dependent weights on the generator level. The signal fit function also includes the normalization to the total number of 226×10^6 produced $B\bar{B}$ pairs, all decay fractions of sequential decays, the B^- lifetime, all MC reconstruction efficiencies, and efficiency corrections derived from control data samples and their MC expectation. Efficiency corrections for track reconstruction and charged particle identification follow those of other recent *BABAR* analyses. For the correction of the π^0 reconstruction efficiency we use a control sample of τ -lepton decays as described below. Small corrections are also applied for deviations of the shapes of the Δm distributions in data and MC because of track resolution differences, and for deviations in the shapes of the $\cos\theta_{\text{BY}}^*$ distributions because of storage-ring energy calibration and resolution.

The background expectation functions are separately determined for 23 classes of backgrounds. This large number of background functions was necessary in order to express each function $B_{i,\tilde{w}}$ as the product of $B_{1,i,\tilde{w}}(\Delta m)$ and $B_{2,i,\tilde{w}}(\cos\theta_{\text{BY}}^*)$. The one-dimensional fit functions $B_{j,i,\tilde{w}}$ are again obtained from fits to MC distributions. The fit to the data has 49 free parameters, in addition to V and ρ^2 there are 47 for adjustments of background normalizations and shapes, Δm shapes, and $\cos\theta_{\text{BY}}^*$ shapes.

Before fitting the expectation function to the data, it is fitted to five different MC subsamples whose size corresponds to the one of the data sample. All five results for V and ρ^2 agree with the MC input by better than one standard deviation. When applied to the data, the fit result is $V = (36.32 \pm 0.60) \cdot 10^{-3}$ and $\rho^2 = 1.146 \pm 0.055$ with a correlation coefficient $\varrho = +0.90$. Integrating $d\mathcal{B}/dw$ over all w leads to $\mathcal{B} = (5.71 \pm 0.08)\%$. The total number of signal events is found to be $23\,499 \pm 329$. Though the fit is maximum-likelihood, a control value of χ^2 can be calculated after the fit as a goodness-of-fit measure. We find 4436.3 for 4095 degrees of freedom which is, purely statistically, 3.8σ too high. Inspecting the distribution of per-bin contributions to χ^2 in all bins

TABLE I: Summary of input parameters.

Input Parameter	Value	Ref.
$\mathcal{B}(Y(4S) \rightarrow B^+B^-)$	$(50.6 \pm 0.8)\%$	[12]
$\mathcal{B}(D^{*0} \rightarrow D^0\pi^0)$	$(61.9 \pm 2.9)\%$	[12]
$\mathcal{B}(D^0 \rightarrow K^-\pi^+)$	$(3.80 \pm 0.07)\%$	[12]
$\mathcal{B}(\pi^0 \rightarrow \gamma\gamma)$	$(98.798 \pm 0.032)\%$	[12]
τ_{B^-}	(1.638 ± 0.011) ps	[12]
$R_1(1)$	1.417 ± 0.075	[6]
$R_2(1)$	0.836 ± 0.043	[6]

of \tilde{w} , Δm , and $\cos\theta_{BY}^*$, we find no concentrations of high values in any area.

Figure shows the result of the fit together with the selected data. The ‘‘Signal’’ part of the fit function contains the correctly reconstructed $B^- \rightarrow D^{*0}e^-\bar{\nu}_e$ decays. The two D^{**} parts contain $B \rightarrow D^{**}e\nu$ decays with (‘‘ Δm peaking’’) and without (‘‘ Δm flat’’) a correctly reconstructed D^{*0} intermediate state ($D^{**} = D_1, D_0^*, D_1', D_2^*, D^*\pi, D\pi$). Events with a correctly reconstructed D^{*0} and a correctly identified electron from the same B and from two different B mesons are in the ‘‘Correlated’’ and ‘‘Uncorrelated’’ background parts, respectively. ‘‘Signal like’’ and ‘‘Uncorrelated’’ background parts, respectively. ‘‘Signal like’’ are true decays $B^- \rightarrow D^{*0}e^-\bar{\nu}_e$ and $\bar{B}^0 \rightarrow D^{*+}e^-\bar{\nu}_e$ which are not correctly reconstructed. The background from true $B \rightarrow D^0e\nu$ decays is called ‘‘ $D^0e\nu$ ’’. All other background candidates from $B\bar{B}$ events (‘‘Combinatorial D^{*0} ’’) are flat in the Δm and the $\cos\theta_{BY}^*$ distribution since they do neither contain a correctly reconstructed D^{*0} nor do they come from a charmed semileptonic decay. The last contribution, only visible in the highest \tilde{w} bins, comes from $c\bar{c}$ events in the continuum.

The systematic uncertainties are divided into analysis-internal and analysis-external ones, see Table II. The former are specific to our analysis, the latter enter by input parameters taken from other measurements. Starting with the internal ones, the relative uncertainty on the efficiency to find a charged particle’s track is 0.8%, leading to 2.4% and 1.2% for \mathcal{B} and V . The dependence of the tracking efficiency on the transverse momentum p_T has an uncertainty which could distort the shape of the \tilde{w} spectrum. The uncertainties arising from the identification of charged tracks as electrons or as kaons contribute to the result as listed under ‘‘particle ID efficiency’’. A significant fraction of the total uncertainty of our result comes from the precision of the π^0 reconstruction efficiency (ϵ_{π^0}). It is determined from $e^+e^- \rightarrow \tau^+\tau^-$ events where one of the two τ leptons is either reconstructed by one track and two clusters (mainly $\tau \rightarrow \rho(\pi\pi^0)\nu$) or it is reconstructed by only one track without clusters (mainly $\tau \rightarrow \pi\nu, \mu\nu\bar{\nu}$) [11]. The other τ , used as a τ -pair tag, is reconstructed in the channel $e\nu\bar{\nu}$. From the numbers of $\tau^+\tau^-$ events reconstructed in each of the two channels we derive an efficiency in data and in MC, giving a cor-

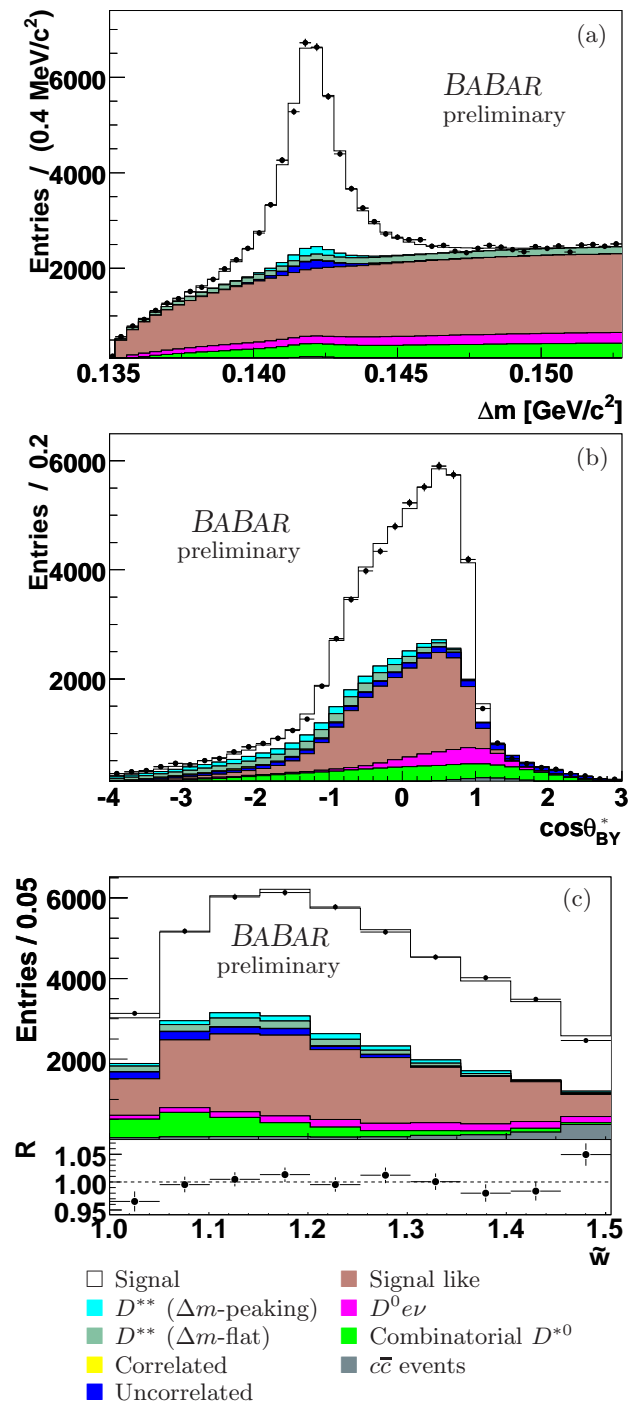


FIG. 1: Data distributions (dots with error bars) and fit results (stacked histograms) for (a) Δm in the $\cos\theta_{BY}^*$ signal range $(-1,+1)$, (b) $\cos\theta_{BY}^*$ in the Δm signal range $(140,144 \text{ MeV}/c^2)$, and (c) \tilde{w} in both signal ranges. The plot below (c) shows the ratio fit/data. The different contributions to the fit function are explained in the text.

TABLE II: Summary of relative systematic uncertainties in percent.

	$\Delta V/V$	$\Delta \rho^2/\rho^2$	$\Delta \mathcal{B}/\mathcal{B}$
tracking efficiency (ϵ_{tr})	1.2	-	2.4
p_T dependence of ϵ_{tr}	0.3	0.5	0.2
particle ID efficiency	0.9	2.0	1.6
extrapolated π^0 efficiency (ϵ_{π^0})	1.8	-	3.6
p_{π^0} dependence of ϵ_{π^0}	1.0	3.5	0.4
Δm shape of D^{**} background	0.1	0.1	0.2
shape parameters	1.0	2.5	0.6
number of $B\bar{B}$ events	0.6	-	1.1
off-peak luminosity	0.1	0.4	<0.1
total internal	2.8	4.8	4.8
$R_1(1)$ and $R_2(1)$	0.1	4.7	0.3
$\mathcal{B}(\Upsilon(4S) \rightarrow B^+B^-)$	0.8	-	1.6
$\mathcal{B}(D^{*0} \rightarrow D^0\pi^0)$	2.3	-	4.7
$\mathcal{B}(D^0 \rightarrow K^-\pi^+)$	0.9	-	1.8
B^- life time	0.3	-	-
D^{**} decay fractions	0.3	0.7	0.3
number of D^{*0} in $c\bar{c}$ events	0.2	0.7	<0.1
total external	2.6	4.8	5.3
total	3.9	6.8	7.2

TABLE III: Derivatives of V , ρ^2 , and \mathcal{B} .

	V	ρ^2	\mathcal{B}
$\partial/\partial R_1$	-0.00038	+0.0303	+0.00382
$\partial/\partial R_2$	-0.00158	-1.22	+0.00551

rection to the simulated π^0 efficiency. The correction is obtained for momenta above 350 MeV/c and has a precision of 3%. We add to this value 2% in quadrature, which is our uncertainty estimate for the extrapolation to the lower-momentum range with all π^0 mesons from $D^{*0}e\nu$ decays. From fit results for different cuts on p_{π^0} we estimate the uncertainty in the shape of the \tilde{w} spectrum which gives one of the major contributions to the uncertainty of ρ^2 (“ p_{π^0} dependence of ϵ_{π^0} ”). Corrections to the Δm shape and to the $\cos\theta_{B\Upsilon}^*$ shape are described by a parametrization of the \tilde{w} dependence which also contributes to the final uncertainties, see “shape parameters”. The determination of the total number of $B\bar{B}$ events in the analyzed data sample has a relative uncertainty of 1.1%. It contributes only to V and \mathcal{B} but not to ρ^2 . The uncertainty on the luminosity of the off-peak data sample propagates also to the final result.

The dominant contribution to the external uncertainty on ρ^2 comes from $R_1(1)$ and $R_2(1)$. We determine the derivatives of our fit result with respect to R_1 and R_2 . We find the values given in Table III leading to the uncertainties listed in Table II. The input decay fractions only contribute to V and \mathcal{B} . An improvement in the precision of $\mathcal{B}(D^{*0} \rightarrow D^0\pi^0)$ would significantly improve our results on V and \mathcal{B} . The uncertainty on the lifetime τ_{B^-}

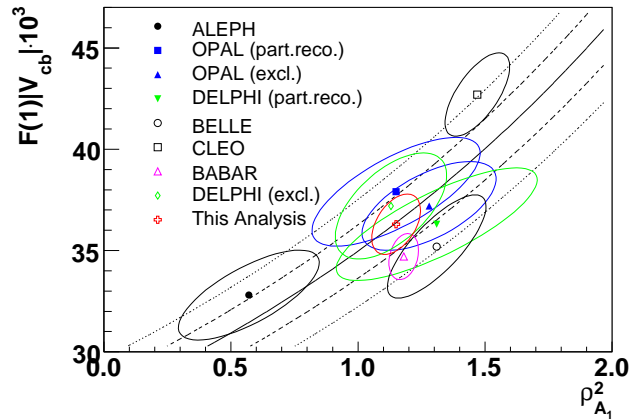


FIG. 2: One-standard-deviation contours (stat. and sys. combined) of V vs. ρ^2 [1] from all recent $\bar{B}^0 \rightarrow D^{*+}e^-\bar{\nu}_e$ results together with our preliminary result. The lines correspond to constant decay fractions $\mathcal{B}(B^- \rightarrow D^{*0}e^-\bar{\nu}_e) = 5.71\% \pm 1\sigma$ and $\pm 2\sigma$ with $\sigma = 0.42\%$.

affects only V . Semileptonic B decays into higher excited charmed mesons, $B \rightarrow D^{**}e\nu$, contribute to the final uncertainties mainly due to their less precisely known decay fractions but also due to their description in the fit. The uncertainty in the number of correctly reconstructed D^{*0} mesons in $e^+e^- \rightarrow c\bar{c}$ events influences \mathcal{B} by less than 0.1%.

Adding all systematic errors in quadrature leads to the last line in Table II and to our preliminary results

$$\begin{aligned}
 F(1) \cdot |V_{cb}| &= (36.3 \pm 0.6 \pm 1.4) \cdot 10^{-3} , \\
 \rho_{A_1}^2 &= 1.15 \pm 0.06 \pm 0.08 , \\
 \mathcal{B}(B^- \rightarrow D^{*0}e^-\bar{\nu}_e) &= (5.71 \pm 0.08 \pm 0.41)\% .
 \end{aligned}$$

The correlation coefficients between $F(1) \cdot |V_{cb}|$ and $\rho_{A_1}^2$ are $\rho = +0.90$ for statistics, $+0.43$ for systematics, and $+0.52$ in total.

Using $F(1) = 0.919 \pm 0.033$ from lattice QCD [13], we obtain $|V_{cb}| = (39.5 \pm 0.6 \pm 2.0) \cdot 10^{-3}$ in good agreement with the average from the exclusive neutral B decays $B^0 \rightarrow D^{*-}\ell^+\nu$, $(39.2 \pm 0.7 \pm 1.4) \cdot 10^{-3}$ [1], and in agreement with results from the inclusive decays $B \rightarrow X_c\ell\nu$, e. g. $(42.0 \pm 0.2 \pm 0.7) \cdot 10^{-3}$ in Ref. [14]. Our result for ρ^2 is in the center of the range (0.5, 1.5) from the $B^0 \rightarrow D^{*-}\ell^+\nu$ experiments [1].

Figure 2 shows the 1σ contour of our result in the $\rho^2, F(1)|V_{cb}|$ plane together with the contours of the neutral- B decays. The quasi-diagonal lines in this Figure are lines of constant decay fraction \mathcal{B} .

For a comparison of our decay-fraction result with the decay fraction of the neutral- B decay mode, we use the lifetime ratio $\tau(B^+)/\tau(B^0) = 1.076 \pm 0.008$ and $\mathcal{B}(B^0 \rightarrow D^{*-}\ell^+\nu) = (5.28 \pm 0.18)\%$ [1]. From this, we expect $\mathcal{B}(B^- \rightarrow D^{*0}\ell^-\bar{\nu}) = (5.68 \pm 0.20)\%$, again in

good agreement with our result. On the other hand, our decay-fraction result is about 1.6σ lower than the PDG average [12] of the B^- results from CLEO and ARGUS [2, 3].

We are grateful for the excellent luminosity and machine conditions provided by our PEP-II colleagues, and for the substantial dedicated effort from the computing organizations that support *BABAR*. The collaborating institutions wish to thank SLAC for its support and kind hospitality. This work is supported by DOE and NSF (USA), NSERC (Canada), CEA and CNRS-IN2P3 (France), BMBF and DFG (Germany), INFN (Italy), FOM (The Netherlands), NFR (Norway), MIST (Russia), MEC (Spain), and STFC (United Kingdom). Individuals have received support from the Marie Curie EIF (European Union) and the A. P. Sloan Foundation.

* Deceased

† Now at Tel Aviv University, Tel Aviv, 69978, Israel

‡ Also with Università di Perugia, Dipartimento di Fisica, Perugia, Italy

§ Also with Università della Basilicata, Potenza, Italy

¶ Also with Universitat de Barcelona, Facultat de Fisica,

Departament ECM, E-08028 Barcelona, Spain

- [1] E. Barberio *et al.* [HFAG Collaboration], arXiv:0704.3575 [hep-ex].
- [2] N. E. Adam *et al.* [CLEO collaboration], Phys. Rev. D **67**, 032001 (2003).
- [3] H. Albrecht *et al.* [ARGUS Collaboration], Phys. Lett. B **275**, 195 (1992).
- [4] For further details see J. Schubert, TU Dresden Dr. rer. nat. Thesis 2006, <http://nbn-resolving.de/urn:nbn:de:swb:14-1169731847466-671>
- [5] I. Caprini, L. Lellouch and M. Neubert, Nucl. Phys. B **530** (1998) 153.
- [6] B. Aubert *et al.* [*BABAR* Collaboration], arXiv:hep-ex/0607076.
- [7] B. Aubert *et al.* [*BABAR* Collaboration], Nucl. Instrum. Meth. A **479**, 1 (2002).
- [8] PEP-II Conceptual Design Report, SLAC-418 (1993).
- [9] Charge-conjugated partners are always implied in this text.
- [10] G. C. Fox and S. Wolfram, Nucl. Phys. B **149**, 413 (1979) [Erratum-ibid. B **157**, 543 (1979)].
- [11] *BABAR* Analysis Document **870**, unpublished.
- [12] W.-M. Yao *et al.* [Particle Data Group], J. Phys. G **33**, 1 (2006).
- [13] S. Hashimoto *et al.*, Phys. Rev. D **66**, 014503 (2002).
- [14] O. Buchmüller and H. Flächer, Phys.Rev. D **73**, 073008 (2006).